Available online at www.eccomasproceedia.org
Eccomas Proceedia COMPDYN (2021) 3617-3632

ECCOMAS
Proceedia

COMPDYN 2021
8th ECCOMAS Thematic Conference on
Computational Methods in Structural Dynamics and Earthquake Engineering
M. Papadrakakis, M. Fragiadakis (eds.)
Streamed from Athens, Greece, 28 - 30 June 2021

ON THE EFFECTIVENESS OF EXPERIMENTALLY-DERIVED FOUNDATION IMPEDANCE FUNCTIONS

C. Amendola[1], F. de Silva[2], D. Pitilakis[1] and F. Silvestri[2]

[1] Dept. of Civil Engineering, Aristotle University of Thessaloniki, Greece
e-mail: {chiaamen,dpitilakis}@civil.auth.gr

[2] University of Naples Federico II, Italy
e-mail: {filomena.desilva,francesco.silvestri}@unina.it

Abstract

In the past decades, several experimental and analytical investigations showed that the dynamic behavior of buildings can be significantly affected by the interaction with a soft foundation soil. In such cases, the actual response of structures founded on shallow foundations can be successfully simulated if the structural model is equipped with springs and dashpots calibrated through frequency-dependent impedance functions. This paper discusses the results of a research project aimed at back-calculating the impedance functions of a shallow square foundation from records of the dynamic behavior of the EuroProteas soil-foundation-structure (SFS) facility, deployed at Euroseistest (Greece). To this aim, forced-vibration tests were executed under different frequencies and increasing loading amplitudes. The experimental impedances were compared with several analytical solutions available in the literature, accounting for different hypotheses on the subsoil model. This comparison improved when the shear wave velocity V_S used to define the analytical functions was reduced accounting for the strain level mobilized by the increasing amplitude of the applied force. A numerical model was realized in the SAP2000 software. The compliance of foundation soil has been introduced using elastic springs, the stiffness of which was calibrated considering either the analytical or the experimental impedances. The fundamental frequency obtained from a modal analysis of the SAP2000 model equipped with the springs calibrated on the experimental impedances turned out to reproduce the fundamental frequency of EuroProteas effectively measured on-site. Such results showed the effectiveness of using experimental impedance functions in the numerical simulations, especially when equivalent soil parameters are hard to define.

Keywords: seismic soil-structure interaction; shallow foundations; forced-vibration tests; dynamic impedance functions

ISSN:2623-3347
Peer-review under responsibility of the organizing committee of COMPDYN 2021.
doi: 10.7712/120121.8734.18958

1. INTRODUCTION

It is customary in design practice to consider the structure fixed at its base, i.e. neglecting the interaction between the soil, foundation and structure (SFSI). Such hypothesis turns out to be realistic only for structures founded on very stiff soil. The up-to-date literature proves that neglecting SFSI effects may lead to an inaccurate evaluation of the actual seismic response of structures founded on soft soil [1]-[4]. The latter, instead, can be realistically simulated considering the deformability of the foundation soil through models endowed at their base through springs and dashpots [5],[6], whose stiffness and damping coefficients are calibrated through the frequency-dependent complex impedance functions.

Several analytical solutions [7]-[9] are available in the literature mostly considering simplified assumptions such as homogeneous soil with elastic behavior. Nevertheless, the equivalent stiffness in a layered soil volume involved in the foundation motion may be hard to define, if the wave velocity profile is not properly measured and accounted for. Moreover, the overburden pressure due to the structural weight can significantly influence the stress-dependent stiffness of the shallowest soil layers and, last but not the least, an increase in the loading force can lead to a non-negligible mobilization of non-linear soil behavior [1],[10]-[12].

In light of these uncertainties, full-scale experimental tests constitute an alternative strategy to evaluated frequency-dependent impedance functions. The earliest on-site studies available in the literature provided impedances for a limited range of frequency [13]-[15] or restricted to specific structures, such as an accelerograph station [16], and a nuclear reactor [17]. More recently, foundation impedance functions were identified from forced-vibration tests executed on a steel frame prototype in California [18] in the frequency range 5-15Hz.

This paper discusses the comparison between theoretical functions accounting for different hypotheses on the soil profile and the frequency-dependent experimental swaying and rocking impedances calculated from full-scale field tests on the single degree of freedom prototype EuroProteas in the EuroSeistest in Greece [19]. The objective of the study is to provide an evaluation on the reliability of field measurements of the impedance functions, in order to overcome the usual simplified assumptions on soil and foundation adopted by the analytical formulations.

2. IMPEDANCE FUNCTIONS

2.1. Definition

Impedances are complex expressions adopted to quantify the soil-foundation reaction when the structure is excited by a harmonic load, Fs, producing a shear force, V, and an overturning moment, M, on the foundation (see Figure 1a). The real part represents the stiffness and the imaginary part the radiation and material damping, which account for the energy scattered and dissipated through hysteresis in the subsoil [8]. When considering the degrees of freedom associated with the foundation swaying and rocking motion, the impedance function is a matrix that links V and M to the foundation displacement, u_f, and rotation, ϑ_f. Moreover, for surface foundations, the out-of-diagonal terms can be neglected [9],[18], hence impedance matrix contains only the two diagonal terms, as follows:

$$\begin{bmatrix} \overline{V} \\ \overline{M} \end{bmatrix} = \begin{bmatrix} \bar{K}_x & 0 \\ 0 & \bar{K}_{\vartheta x} \end{bmatrix} \begin{bmatrix} \overline{u_f} \\ \overline{\vartheta_f} \end{bmatrix} \tag{1}$$

The terms of the impedance matrix are generally presented in the literature in the following explicit form:

$$\bar{K}_j = k_j(a_0) K_j + i\omega c_j(a_0) C_j \tag{2}$$

where $j=x$ for the horizontal vibration and $j=\vartheta x$ for rocking motion. The static stiffness K_j, and the dashpot coefficient, C_j, depend on the soil shear modulus, G, and Poisson's ratio, ν, as well as on a characteristic dimension of the foundation (radius r or foundation half-width B). The dynamic coefficients, $k_j(a_0)$ and $c_j(a_0)$, depend on the vibration frequency, ω, the characteristic dimension of the foundation, r, and the soil shear wave velocity, V_S, through the frequency factor, $a_0=\omega r/V_S$.

Eqs. (1) can be solved in the frequency domain from the dynamic equilibrium of the structure-foundation system depicted in Figure 1b, as described by [19].

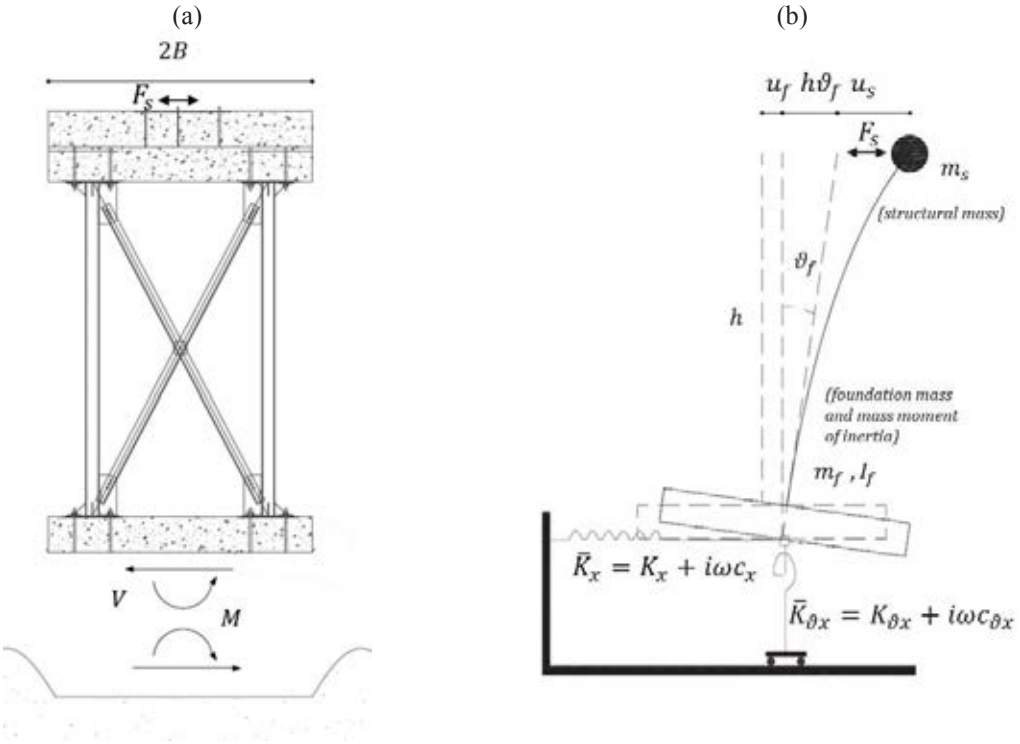

Figure 1: (a) Schematic view of the EuroProteas facility during forced vibration tests and associated reaction in the soil; (b) in-plane motion model of the single-degree-of-freedom system placed on translational and rotational springs adopted for the interpretation of experimental data. Modified after [19].

2.2. Analytical impedances

Different analytical functions are available in the literature for the real and complex impedance components, mostly referring to simplified conditions such as rigid massless foundation, more or less embedded in a subsoil which is typically assumed as an elastic homogeneous half-space [9],[10]. Nevertheless, [11],[20] suggest that the effect of soil inhomogeneity can be approximated with an equivalent halfspace with representative values of V_S and damping ratio averaged over depths equal to $0.75r_{\vartheta x}$ and $0.75r_x$, where $r_{\vartheta x}$ and r_x are the

rocking and swaying equivalent radii. Other widespread solutions (e.g. [21]) assume non-uniform soil profiles, including the case of a shallow layer stiffer or softer than the underlying halfspace [22]. Finally, non-linear soil behavior can play a crucial role under moderate to strong motions leading to a variation in the impedance functions. More recently, [23] introduced the effects of non-linear behavior, through a series of iterative linear analyses by updating the shear modulus and damping ratio consistently with the strain level induced by different excitation amplitudes. Reduction coefficients are then provided to reduce the real and imaginary parts of the analytical impedances by [9] when the excitation levels range from 0.01g to 1g.

Table 1 lists the analytical solutions and the associated hypotheses on the subsoil model adopted in this study to characterize the analytical impedance functions used for comparison with the experimental impedances back-calculated by [19]. The classic solution by Pais and Kausel [9] for a homogenous elastic halfspace was firstly selected for comparison; these equations are very similar to the widespread expressions given by [8] which therefore were not considered. Then, among all the different combinations of shear moduli of the layer and halfspace by Liou [22], a 50% reduction was considered between the shear moduli of the half-space medium and that of the foundation deposit layer (i.e. G_2/G_1=0.5). Finally, the solution by [23], accounting for soil nonlinearity, was checked. The dynamic coefficients corresponding to 0.01g and 0.2g were multiplied for the static stiffness expressions provided by [9].

Authors	Year	Soil
Pais and Kausel [9]	1988	Homogeneous elastic halfspace
Liou [22]	1993	Viscoelastic layer (G_1) on a homogeneous halfspace (G_2), G_2/G_1=0.5
Pitilakis et al. [23]	2013	Homogeneous equivalent linear (0.01g and 0.2g) halfspace

Table 1 Analytical impedance functions and associated subsoil models used for comparison with experimental data.

3. EXPERIMENTAL TESTS ON THE SISIFO PROJECT

3.1. Experimental facility: EuroProteas in the Euroseistest

The above theoretical impedance functions were compared with the experimental results of the research project "Seismic Impedance for Soil-structure Interaction From On-site tests, SISIFO", funded by the HORIZON2020-supported program SERA the Seismology and Earthquake Engineering Research Infrastructure Alliance for Europe (http://www.sera-eu.org/en/home/). The SISIFO project aimed to investigate the effectiveness of different procedures of experimental identification of the impedance functions at prototype scale. For this reason, on-site tests were performed on the full-scale experimental facility of EuroProteas (Figure 2a) in the Euroseistest TST site located in the middle of Mygdonian valley in Northern Greece (Figure 2b).

EuroProteas consists of a simple steel frame supported by a 3m x 3m x 0.4m foundation raft, overtopped by two interconnected slabs each one of them identical to it (Figure 2a). The steel frame consists of four squared hollow steel columns (QHS 150mm x 150mm x 10mm) clamped on the foundation through steel bolts. L-shaped cross-braces (100mm x 100mm x 10mm) rigidly connect the steel columns all around the structure. The raft can be considered as an ideal ‘shallow foundation’ since the surrounding soil was intentionally removed before the execution of the tests discussed in the following. More details on the structural features are discussed by [19] and [24].

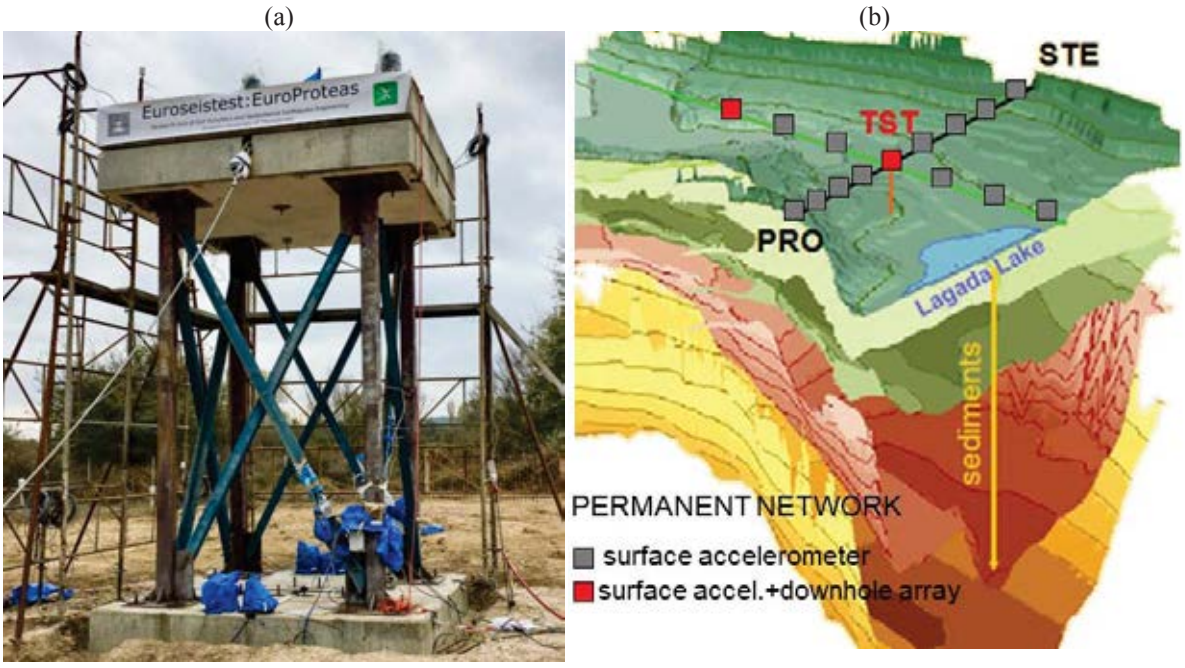

Figure 2 (a) Full-scale experimental facility of EuroProteas located (b) in the TST site, in the middle of the EuroSeistest.

The foundation subsoil was investigated and its dynamic properties were defined on the basis of extended geophysical and geotechnical in-situ and laboratory surveys reported in earlier studies [24]-[27]. The soil profile is composed of a first layer of silty-clayey sand about 7m thick, a layer of clayey-silty sand with local contents of gravel between 7m and 22m, and the last layer of marly silt and silty sand down to a depth of 30m. The shear wave velocity of the uppermost 6m was found to vary between 150m/s, as resulting from a DH test, and 100m/s, from the interpretation of further geophysical tests (see Figure 3a).

All the V_S profiles shown in Figure 3a refer to free-field investigations performed before the construction of the prototype. However, it must be observed that the increment of the mean effective stress due to the structural weight may have caused an increase in the initial shear stiffness at the shallowest depths [28]. Therefore, as suggested by [11],[18], the free-field velocity ought to be corrected to account for such a stiffening, by multiplying V_S for an overburden correction factor (hereafter *OCF*) which can be computed as follows:

$$OCF = \left(\frac{\sigma_v^{'}(z) + \Delta\sigma_v^{'}(z)}{\sigma_v^{'}(z)} \right)^{n/2} \tag{3}$$

where $\sigma_v^{'}(z)$ and $\Delta\sigma_v^{'}(z)$ are the effective vertical lithostatic stress and its increment due to the structural weight, n is an exponent increasing with soil plasticity index [29],[30]. Figure 3b reports the variation of *OCF* with depth between z=0.1m and z=6m (black solid line), calculated assuming n=0.5 and adopting the Steinbrenner's solution for the vertical stress increment [31]. As expected, *OCF* is maximum at the foundation level and sharply decreases with depth. Previous studies in the literature [20] suggest to correct V_S profiles for *OCF* values averaged through appropriate depth intervals, in order to obtain a mean equivalent velocity profile. Following such a suggestion, Figure 3b also reports the values of *OCF* averaged over 50% (red solid line) and 100% (blue solid line) of the foundation width, i.e. 2B.

The average increase of the free-field V_S is estimated to be equal to 35% ($\overline{OCF}_B$=1.35) up to the foundation half-width, B, and 22% ($\overline{OCF}_{2B}$=1.22) up to the total foundation dimension, 2B. It follows that the actual velocity profile may present an inversion, with a greater value of V_S in the shallowest range of depths (i.e., that most interested by the foundation rocking motion) with respect to the soil volume mobilized by the foundation swaying.

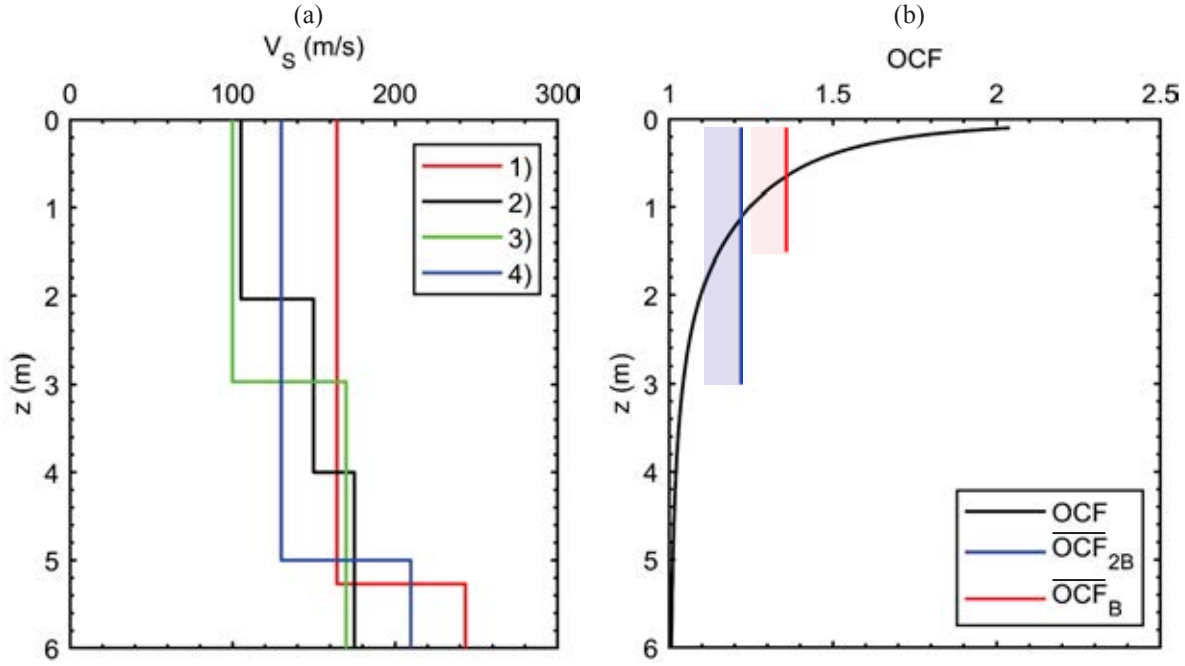

Figure 3 (a) Shear wave velocity profiles from 1) down-hole test before EuroProteas construction, 2) at a site approximately 50m away from the facility [25], 3) reference model of the valley cross-section from updated geophysical, geotechnical and numerical modeling [26], 4) profile from detailed geotechnical and geophysical surveys [27], as adapted from [24]; (b) overburden correction factor, *OCF*, for the EuroProteas foundation soil and its average along the foundation half-width, B, and width, 2B.

3.2. Instrumentation layout and performed tests

The facility was instrumented with triaxial accelerometers (CMG-5TD and CMG-5TCDE, Guralp Systems Ltd) to record both the structural and the foundation response (Figure 4). In particular, the instrumentation layout consists of 5 accelerometers mounted on the roof, three along the axis parallel to the direction of shaking (in-plane) and two at the opposite corners of the slab, to capture possible out-of-plane motion. Additionally, four triaxial accelerometers were mounted in pairs at the opposite edges of the foundation slab along the direction of shaking, in order to ensure and validate the proper recording of the foundation's translational and rotational response. All the instruments were connected to external global positioning system (GPS) antennas and their sampling frequency was set to 200Hz. They were oriented along the positive x-direction of loading, which forms an angle of 30 degrees with the magnetic North. However, for sake of simplicity, the x and the y component of each record were tagged as North and East, respectively, as shown in Figure 4.

The dynamic response of the instrumented facility was firstly identified under random ambient noise test, in which the structural response was recorded with no external excitation. Free-vibration tests were also carried out by a ‘snap-back’ procedure, in which the roof was initially slightly displaced and thereafter released to induce the free vibration of the prototype structure (see [19]). The structure was then subjected to sinusoidal forced vibration tests, by

changing the frequency in a range of interest of earthquake engineering, i.e. from 1Hz to 10Hz, through a shaker mounted on the roof slab. The MK-500U (ANCO Engineers Inc) eccentric mass vibrator system was adopted as a source of harmonic excitation. The following equation controls the generated harmonic load:

$$F_s = E\left(2\pi f\right)^2 \sin\left(2\pi ft\right) \tag{4}$$

The frequency of the shaker force was held constant until the system reached the steady state. Four different forced vibration test series were executed, by changing the frequency of the excitation and adjusting the rotating mass through the vibrator's eccentricity of the shaker. Each applied frequency was locked for 60s and then incremented by 1Hz steps in the range 1Hz – 10Hz. The frequency step was reduced to 0.5Hz when approaching the first vibration mode, in order to more accurately record the resonance response.

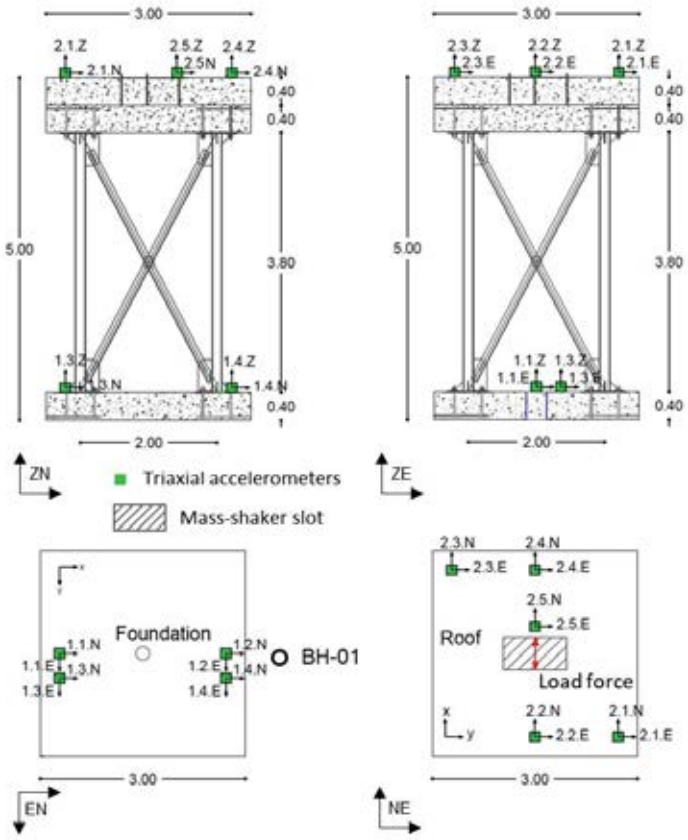

Figure 4 Instrumentation layout of the facility during the forced vibration tests.

Table 2 reports the details of the lowest and highest force amplitude tests, i.e. Forced-A and Forced-D, yielding the experimental impedance functions which were taken for comparison with the analytical solutions listed in Table 1.

Experiment	Frequency range $f=\omega/2\pi$	Force range (min-max) $E\omega^2$
(-)	(Hz)	(kN)
Forced-A	1-2-3-3.5-4-4.5-5-6-7-8-9-10	0.07-7.30
Forced-D	1-2-2.5-3-3.5-4-5-6-7-8	0.45-28.58

Table 2 Force and frequency range applied during Forced-A and Forced-D tests.

3.3. Experimental impedance functions

As detailed in [19], experimental impedance functions were back-calculated through Eqs. (1) from the data recorded during the forced vibration tests. The left side of the system of Eqs. (1) are the shear force, V, and the overturning moment, M, acting on the foundation. In the time domain, they result from the difference between the applied loads (F_s and $F_s h$) and the inertia forces generated by the structural mass, m_s, the foundation mass, m_f, and its mass moment of inertia, I_f. The computational details are reported in [19] and here omitted for sake of brevity. The right side of Eqs. (1), i.e. the displacement array, defines the motion of the rigid foundation slab by two independent swaying, u_f, and rocking, ϑ_f, kinematic components.

The foundation rocking, ϑ_f, was computed as the difference between the double integration of vertical records 1.3Z and 1.4Z, divided by their distance. The foundation swaying, u_f, was calculated from the displacement obtained by integrating the acceleration recorded by sensor 1.4N minus the displacement induced by the foundation rocking, i.e. $\vartheta_f h_f$. The applied force defining the load vector was calculated according to Eq. (4), where the phase angle, φ, between the applied force itself and the response was assumed to equal to that characterizing the force-displacement time shift of a simple SDOF oscillator [32] with the overall damping $\xi=5\%$ and the natural frequency f_n = 3.4Hz for Forced-A and 3.0Hz for Forced-D which were inferred from the interpretation of noise and snap-back tests [19].

Figure 5 shows the real part of impedance functions calculated in [19] from Forced-A (full circles) and Forced-D (hollow circles) tests, for both swaying and rocking motions. As it can be observed from the plots, both swaying and rocking dynamic stiffness decrease with the increment of the excitation force, i.e. from Forced-A to –D, apparently due to the mobilization of non-linear soil behavior.

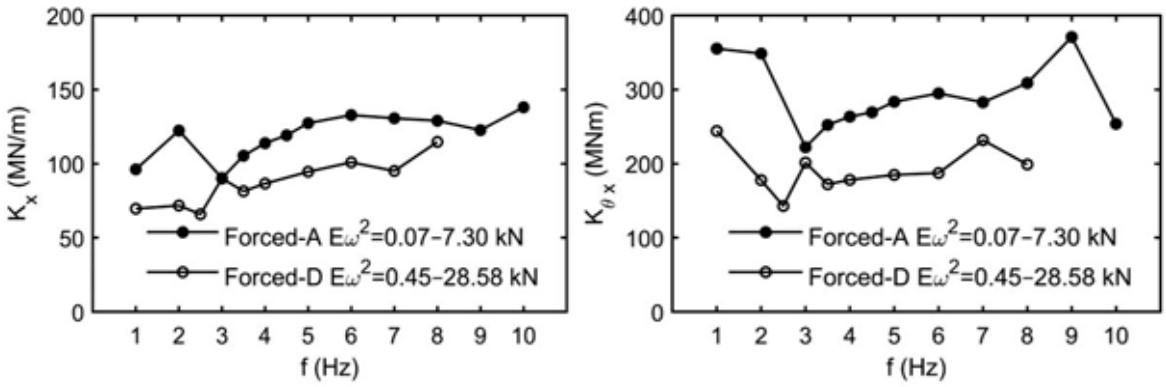

Figure 5 Comparison between the real part of impedance functions back-calculated from Forced-A (full circles) and Forced-D (hollow circles) vibration tests for swaying and rocking motion

3.4. Evidence of non-linear soil behavior from the experimental data

Mobilization of nonlinearity in the soil leads to a decrease of soil stiffness and to an increase of hysteretic damping, consequently modifying the foundation motion. For such a reason, soil properties defining impedance functions must be selected to properly account for the mobilized shear strain levels. An estimate of the peak shear strain amplitude, $\gamma_{eff\,\max}$, can be obtained from the ratio between the peak horizontal velocity recorded on the foundation, $\dot{u}_f$, and the shear wave velocity, V_S [33],[34].

The resulting mobilized shear strains during the Forced-A and -D tests are reported in Figure 6a. As expected, the strain amplitude increases with the level of the applied force, i.e. from Forced-A to -D. The system reaches the highest peak shear strain close to the resonance of the facility, i.e. around 3.0 and 2.5Hz, respectively under the Forced-A and -D tests [19],[35]. In correspondence of these values, $\dot{u}_f$ resulted equal to 0.25cm/s and 0.9cm/s, which combined to a V_S equal to 100 m/s (see Figure 3a), yields to $\gamma_{eff\,\max}$ of the order of 0.0025% for Forced-A (blue hexagon in Figure 6a) and 0.009% for Forced-D (red hexagon in Figure 6) respectively. Figure 6b shows the variation of normalized shear modulus with the shear strain resulting from a resonant column test (reported in [24]) on a sample taken at a depth between 2.7m and 3.0m, from the borehole BH-01 close to the foundation. The plot revealed that the peak shear strain $\gamma_{eff\,\max}$ estimated for the Forced-A test is associated with a negligible reduction of the shear modulus, while $\gamma_{eff\,\max}$ for the Forced-D test produces a reduction of the shear modulus of the order of 25% of its initial value. Hence, soil nonlinearity is expected to affect rather significantly the experimental impedances derived from the Forced-D test.

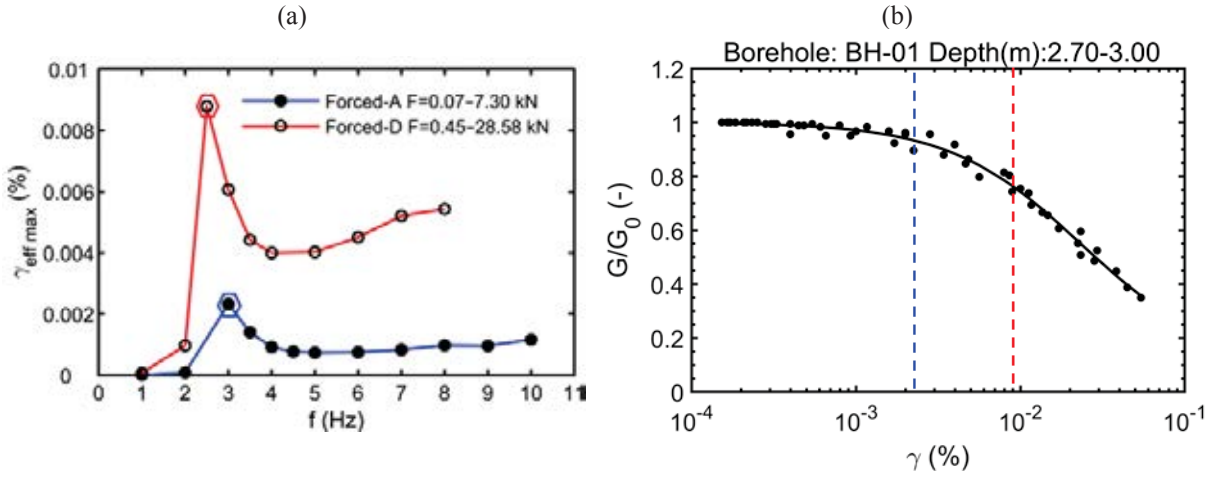

Figure 6 (a) Effective peak shear strain mobilized during Forced-A (full circles connected with a blue solid line) and Forced-D (hollow circles connected with a red solid line) tests, with resonance peaks highlighted by a blue and red marker, respectively; (b) peak strain amplitudes drawn with the same colors across the shear modulus reduction curve G/G_0 (as adapted from [24]).

4. CALIBRATION OF ANALYTICAL SOLUTIONS AGAINST ON-SITE IMPEDANCE FUNCTIONS

The best-fitting between the analytical and experimental impedances was investigated by changing the V_S value in the computation of the analytical value until the difference with the experimental impedance was minimized. Being both the impedances variable with frequency (see for instance Figure 5) the V_S was computed by minimizing the sum of the squares of the residuals (or offsets), defined as the difference between the analytical (K_{anal}) and experimental (K_{exp}) real part of impedances as follows:

$$RSS=\sum_{i=1}^{n}\left(K_{exp\,i}-K_{anal\,i}(V_s)\right)^2 \tag{5}$$

where i indexes the frequencies listed in Table 2.

The resulting *RSS* normalized with respect to the maximum value, i.e. that associated with $K_{\vartheta x}$ under the test Forced-A, are reported in Table 3 along with the best-fitting V_S values.

	Forced-A					Forced-D				
	swaying (K_x)		rocking ($K_{\theta x}$)			swaying (K_x)		rocking ($K_{\theta x}$)	
	Vs m/s	*RSS* %	*Vs* m/s	*RSS* %		*Vs* m/s	*RSS* %	*Vs* m/s	*RSS* %
Pais and Kausel	89	6	99	100	Pais and Kausel	77	5	81	34
Liou (G_2/G_1=0.5)	96	3	98	57	Liou (G_2/G_1=0.5)	83	2	79	20
Pitilakis et al. (0.01g)	92	6	96	68	Pitilakis et al. (0.2g)	95	3	96	34

Table 3 Minimum dimensionless values of Residual Sum of Squares (*RSS*) associated with the shear wave velocity (V_S) used to define the best-fitting analytical function for the swaying and rocking dynamic stiffness back-calculated after Forced-A and Forced-D tests.

The best-fit analytical stiffness is compared in Figure 7a for the swaying and in Figure 7b for the rocking motion to the experimental data of Forced-A (left) and Forced-D (right) tests.

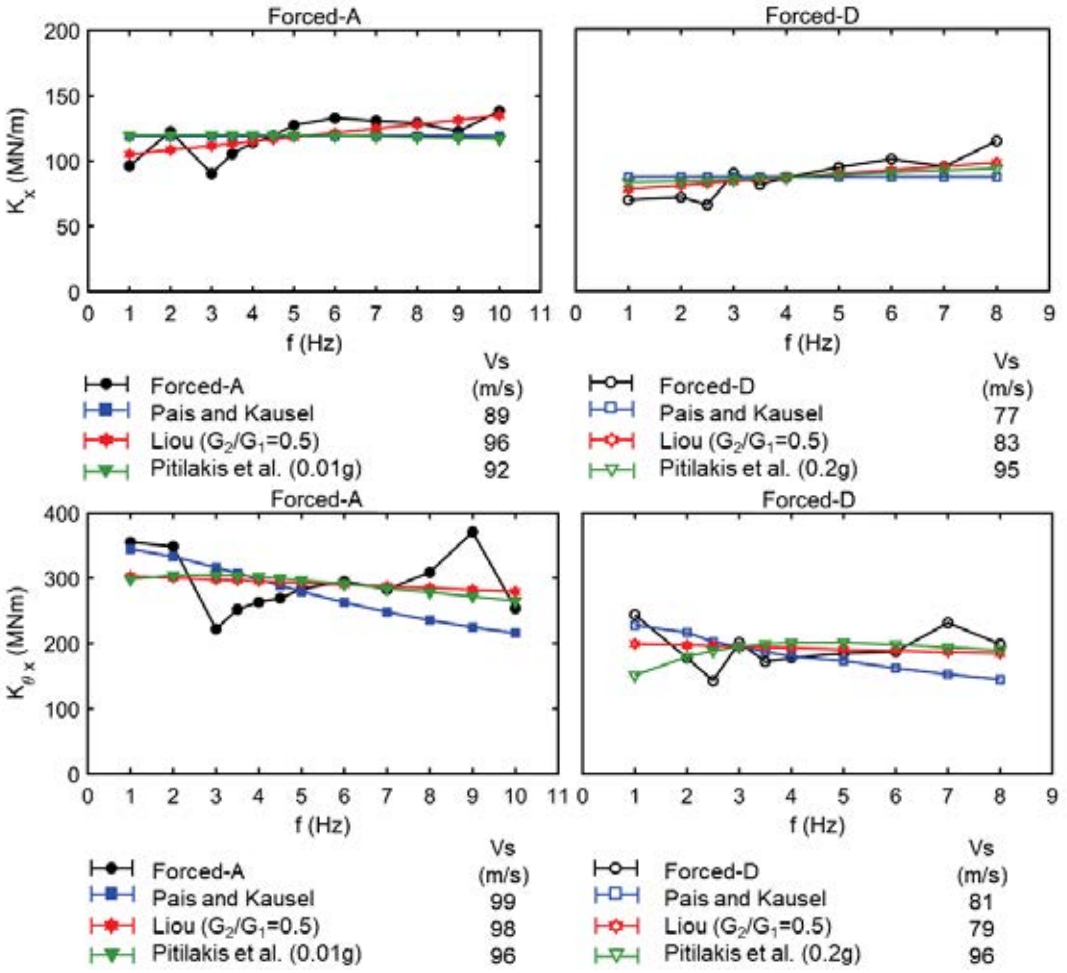

Figure 7 Comparison between the real part of experimental and analytical functions accounting for different values of shear wave profile for the foundation (a) swaying and (b) rocking for (left) Forced-A and (right) Forced-D tests.

For a given analytical solution, the best-fitting V_S depends on the considered foundation motion. With reference to the results of the Forced-A test, the highest discrepancy is observed for the solution by Pais and Kausel [9], which requires a V_S =89 m/s to match the experimentally derived swaying impedance and a V_S =99 m/s (i.e. with an increase of 11% with respect to the swaying) to match the rocking component. As it is well known [20],[36], the soil depth involved by foundation rocking is almost equal to the foundation half-width and that associated with the swaying motion to the foundation width. Hence the stiffness increase due to the EuroProteas overburden is expected to affect the rocking more than the swaying motion. As shown in Section 3.1 and Figure 3b, the relative difference between the OCF averaged up to the foundation halfwidth and width, $\overline{OCF}_B$ and $\overline{OCF}_{2B}$, is exactly equal to 11%, i.e. that between the V_S values required to fit the rocking and swaying motions.

From a visual analysis of Figure 7 it appears that the best overall agreement between analytical solutions and experimental data (black symbols) is reached when considering the heterogeneous subsoil profile proposed by Liou [22] (red symbols). As reported in Table 3, such analytical impedances are associated with the lowest RSS for both swaying and rocking modes. Conversely, when considering analytical functions under simplified assumptions such as homogenous soil model (i.e. Pais and Kausel [9]), the match with experimental functions worsens (blue symbols) and the greatest RSS values are reached.

Both Table 3 and Figure 7 show that the "best fitting" shear wave velocity reduces when considering the Forced-D tests. Table 4 lists the ratio between the V_S used to define the analytical expressions for the best-fitting of Forced-D test results and the corresponding value for the Forced-A, for the two considered foundation motions.

	$V_{S\,\text{Forced-D}}/V_{S\,\text{Forced-A}}$	
	swaying	rocking
Pais and Kausel[9]	0.86	0.82
Liou (G_2/G_1=0.5)[22]	0.86	0.81
Pitilakis et al. [23]	1.03	1.00

Table 4 Shear wave velocity reduction from Forced-A to Forced-D, for both swaying and rocking motions.

The normalized shear wave velocity reduction ranges between 14% and 19% when adopting Pais and Kausel [9] and Liou [22] solutions. Such values are coherent with the experimental data reported in Figure 6b, revealing a reduction of the normalized shear modulus up to 25%, hence a V_S reduction up to 13%. When soil nonlinearity is directly considered in the analytical solution, as suggested by Pitilakis et al. [23], the best-fitting V_S is the same for the Forced-A and Forced-D tests, since soil properties consistent with the level of shear strain induced by shaking (i.e. 0.01g and 0.2g) are considered by the approach itself.

Finally, it is worth highlighting that the value of V_S matching the Forced-D test is less affected by the foundation motion than those matching the Forced-A. This is due to the fact that rocking motion mobilizes higher strain levels concentrated in the very shallow foundation soil, reducing its stiffness. Hence the initial inversion induced by the structural weight (see Section 3.1) is reduced, making the stiffness in the soil volume affected by the rocking and swaying motions more homogeneous.

5. NUMERICAL SIMULATION

A numerical simulation (Figure 8) with the finite element software SAP2000 allowed to determine the fixed-base (FB) and compliant-base (CB) dynamic response of the prototype.

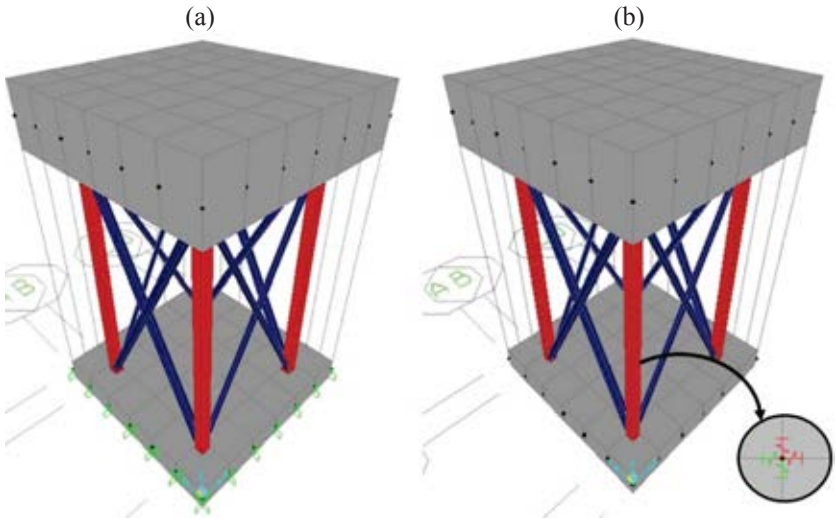

Figure 8 Numerical model for (a) the fixed-base, FB, and (b) compliant-base, CB, prototype.

Following the substructure approach, the numerical simulation of the compliant-base model, CB, was performed by restraining the base of the structural model with a system of springs. Their translational and rotational stiffness values were firstly characterized from the real part of the 'linear' experimental impedances, as resulting from Forced-A test for both swaying and rocking modes, with reference to the fundamental frequency of the system, i.e. 3Hz (see [19]), as in the usual procedure. To highlight the effectiveness of using experimental functions, the analysis was repeated by considering each analytical function listed in Table 1. In such a case, the calibration procedure followed in Section 4 was ignored and the shear wave velocity was assumed from the free-field measurements in Figure 4, as commonly done in lack of experimental impedance values. The minimum value of the range 100m/s - 150m/s of V_S measured in the uppermost 3 m of the layered soil profile was assumed, i.e. 100 m/s (Figure 3).

Results of modal analyses performed on the fixed-base and compliant-base models are reported in Table 5. They confirmed the expected strong influence of the soil-structure interaction on the dynamic response of the facility. In all cases, the fundamental frequency is significantly lower than the value of 9.13Hz resulting from the fixed-base model. Only when characterizing the springs with the experimental impedances, the results of the modal analysis were consistent with the on-site measurements, identifying a fundamental frequency around 3.0Hz under the Forced-A test. Such evidence highlights that the calibration of the compliant-base model through experimental impedances is possible and is even more accurate than the traditional analytical impedance functions because it implicitly accounts for soil inhomogeneity and nonlinearity, which are either neglected or hard to be quantified in the definition of analytical formula.

Foundation restraining system	frequency (Hz)	period (s)
FB (Fixed-base)	9.13	0.11
CB (Forced-A)	3.05	0.33
CB (Pais and Kausel [9])	3.11	0.32
CB (Liou (G_2/G_1=0.5) [22])	3.38	0.30
CB (Pitilakis et al. (0.01g) [23])	3.44	0.29

Table 5 Fundamental frequency and period associated with the dominant response of the structure for the fixed-base and compliant-base conditions, considering experimental and analytical impedance functions.

6. CONCLUSIONS

The response of a structure resting on soft soil conditions may be different compared to the fixed-base assumption. In the up-to-date literature, SFSI is incorporated in the analysis of shallow foundations using the uncoupled 'substructure method'. The foundation compliance is taken into account through frequency-dependent impedance functions.

Several analytical functions are available in the literature depending on soil and foundation properties, varying with depth and strain level. In this study, theoretical functions accounting for different hypotheses on the subsoil model were calibrated against the impedance functions of a shallow square foundation back-figured from records of the dynamic behavior of the EuroProteas soil-foundation-structure (SFSI) facility, in the framework of the SISIFO project.

The experimental impedances evaluated under different values of forces applied by the shaker match reasonably well with the analytical frequency-dependent impedance functions calculated for varying shaking levels when changing the foundation soil properties according to the mobilized shear strain.

In this study, the agreement was found to increase considerably when considering an inversion in the soil velocity profile, as for the theoretical impedances proposed by Liou [22]. Such an effect is probably due to the increase of shear stiffness induced by the overburden pressure. To overcome the above limitation, future experimental campaigns addressed to evaluate impedance functions should include shear wave measurements after the installation of the prototype, for instance by means of a hole across the foundation slab, allowing for the execution of down-hole or cross-hole tests.

Moreover, when increasing the frequency-dependent amplitude of the force applied through the shaker, significant non-linear effects are induced; for such a reason, laboratory tests on specimens representative of the soil beneath the foundation are needed to investigate the role of inelastic soil behavior even at the lowest strain levels.

A numerical simulation in the SAP2000 software confirmed the effectiveness of using experimental impedance functions, especially when the soil parameters are hard to be defined. The comparison among the obtained predominant frequencies of the model equipped with springs calibrated on the experimental and analytical functions highlighted that the fundamental frequency of EuroProteas measured on-site is well-reproduced only if the experimental impedances are adopted in the analysis.

In conclusion, measurement of the foundation impedance can be a sound alternative strategy with respect to the predictive formulae. It does not require over-simplified assumptions on the geometrical and mechanical properties of both foundation and subsoil.

7. ACKNOWLEDGMENT

The Authors acknowledge support by the project “Seismology and Earthquake Engineering Research Infrastructure Alliance for Europe (SERA)". This project has received funding from the European Union’s Horizon 2020 research and innovation programme under grant agreement No. 730900. The first Author has received fundings from the European Union’s H2020 research and innovation programme under the Marie Sklodowska-Curie grant agreement N° 813137, project URBASIS. OASP-ITSAK is also acknowledged for providing part of the instrumentation and manpower for the execution of the tests.

8. REFERENCES

[1] G. Mylonakis, G. Gazetas, Seismic soil-structure interaction: Beneficial or detrimental?, *Journal of Earthquake Engineering*, 4(3), 277–301, 2000.

[2] R. Paolucci, Soil-structure interaction effects on an instrumented building in Mexico City. *European Earthquake Engineering*, 3, 33-44, 1993.
[3] A. Piro, F. de Silva, F. Parisi, A. Scotto di Santolo, F. Silvestri, Effects of soil-foundation-structure interaction on fundamental frequency and radiation damping ratio of historical masonry building sub-structures. *Bulletin of Earthquake Engineering*, 18, 1187–1212, 2019.
[4] F. de Silva, Influence of soil-structure interaction on the site-specific seismic demand of masonry towers. *Soil Dynamics and Earthquake Engineering*, 131, 2020.
[5] A.S. Veletsos, J.W. Meek, Dynamic behavior of building-foundation systems. *Earthquake Engineering & Structural Dynamics*, 3(2),121–138, 1974.
[6] A.S. Veletsos, V.V. Nair, Seismic interaction of structures on hysteretic foundations. *Journal of Structural Engineering*, 101, 109-129, 1975.
[7] A.S. Veletsos, B. Verbic, Vibration of viscoelastic foundations. *Earthquake Engineering & Structural Dynamics*, 2, 87–102. 1973.
[8] G. Gazetas, Formulas and charts for impedances of surface and embedded foundations. *Journal of Earthquake Engineering*, 117(9), 1363–81, 1991.
[9] A. Pais, E. Kausel, Approximate formulas for dynamic stiffnesses of rigid foundations. *Soil Dynamics and Earthquake Engineering*, 7(4), 213–27, 1988.
[10] G. Gazetas, Analysis of machine foundation vibrations: state of the art. *Soil Dynamics and Earthquake Engineering*, 2(1), 2–42, 1983.
[11] NIST, Soil-structure interaction for building structures. *Technical report*, US Department of Commerce, Washington, DC, 2012.
[12] A. Di Tommaso, R. Lancellotta, D. Sabia, D. Costanzo, F. Focacci, F. Romaro, Dynamic identification and seismic behaviour of the Ghirlandina tower in Modena (Italy). *Proceedings of the AGI International Conference: Geotechnical Engineering for the Preservation of Monuments and Historic Sites*. Bilotta E., Lirer S., Viggiani C. (eds), Napoli, May 30-31 2013. 343-351, Taylor & Francis Group, London. ISBN 978-1-138-00055-1.
[13] J.E. Luco, M.D. Trifunac, H.L.Wong, Isolation of soil-structure interaction effects by full-scale forced vibration tests. *Earthquake Engineering & Structural Dynamics*, 16, 1-21,1988.
[14] A.N. Lin, P.C. Jennings, Effect of embedment on foundation-soil impedance. *Journal of Engineering Mechanics*, 110(7), 1060-1075, 1984.
[15] H.L. Wong, M.D. Trifunac, J. A. Luco, Comparison of soil-structure interaction calculations with results of full-scale forced vibration tests. *Soil Dynamics and Earthquake Engineering*, 7(1), 22-31, 1988.
[16] C.B. Crouse, G.C. Liang, G.R. Martin, Experimental study of soil-structure interaction at an accelerograph station. *Bulletin of the Seismological Society of America*, 74(5), 1995-2013, 1984.
[17] F.C.P. de Barros, J.E. Luco, Identification of foundation impedance functions and soil properties from vibration tests of the Hualien containment model. *Soil Dynamics and Earthquake Engineering*,14, 229–48, 1995.
[18] S. Tileylioglu, J.P. Stewart, R.L. Nigbor, Dynamic stiffness and damping of a shallow foundation from forced vibration of a field test structure. *Journal of Geotechnical and Geoenvironmental Engineering*, 137(4), 344–53, 2011.
[19] C. Amendola, F. de Silva, A. Vratsikidis, D. Pitilakis, A. Anastasiadis, F. Silvestri, Foundation impedance functions from full-scale soil-structure interaction tests. *Soil Dynamics and Earthquake Engineering*,141, 106523, 2021.

[20] J. Stewart, S. Kim, J. Bielak, R. Dobry, M. Power, Revisions to soil structure interaction procedures in NEHRP design provisions. *Earthquake Spectra*, 19(3), 677-696, 2003.
[21] H.L. Wong, J.E. Luco, Tables of impedance functions for square foundations on layered media. *International Journal of Soil Dynamics and Earthquake Engineering*, 4(2), 64–81, 1985.
[22] G.S. Liou Impedance for rigid square foundation on layered medium. *Structural Engineering/Earthquake Engineering*, 10(2), 83-93,1993.
[23] D. Pitilakis, A. Modaressi-Farahmand-Razavi, D. Clouteau, Equivalent-linear dynamic impedance functions of surface foundations. *Journal of Geotechnical and Geoenvironmental Engineering*,139(7), 1130-1139, 2013.
[24] D. Pitilakis, E. Rovithis, A. Anastasiadis, A. Vratsikidis, M. Manakou, Field evidence of SFSI from full-scale structure testing. *Soil Dynamics and Earthquake Engineering*, 112, 89–106, 2018.
[25] D. Raptakis, N. Theodulidis, K. Pitilakis, Data analysis of the euroseistest strong motion array in Volvi (Greece): standard and horizontal-to-vertical spectral ratio techniques. *Earthquake Spectra*,14(1), 203–24, 1998.
[26] K. Pitilakis, D. Raptakis, K. Lontzetidis, Th. Tika-Vassilikou, D. Jongmans. Geotechnical & geophysical description of EURO-SEISTEST, using field, laboratory tests and moderate strong-motion recordings. *Journal of Earthquake Engineering*, 3(3), 381–409, 1999.
[27] D.G. Raptakis, F.J. Chavez-Garcıa, K. Makra, K. Pitilakis. Site effects at Euroseistest-I. Determination of the valley structure and confrontation of observations with 1D analysis. *Soil Dynamics and Earthquake Engineering*, 19(1), 1–22, 2000.
[28] B.O. Hardin, The nature of stress-strain behavior for soils. *Geotechnical Engineering Division Specialty Conference on Earthquake Engineering and Soil Dynamics*, ASCE, Pasadena (California), 1978.
[29] C. Mancuso, F. Silvestri, F. Vinale, Soil properties relevant to seismic microzonation. *Proc. I Japanese-Turkish Conference on Earthquake Engineering*, Istanbul. Istanbul Technical University and Chamber of Civil Engineers, 1997.
[30] A. d'Onofrio, F. Silvestri, Influence of micro-structure on small-strain stiffness and damping of fine grained soils and effects on local site response. *Proc. IV International Conference on 'Recent Advances in Geotechnical Earthquake Engineering and Soil Dynamics*', S. Diego, 2001.
[31] W. Steinbrenner, A rational method for determination of the vertical normal stresses under foundations, *Proceedings of the International Conference on Soil Mechanics and Foundation Engineering*, Cambridge, Massuchusetts, 142-143, 1936.
[32] A.K. Chopra, Dynamics of Structures: *Theory and applications to earthquake engineering. 3th Edition* New Jersey, USA: Prentice Hall Inc, 2003.
[33] L.M. Star, S. Tileylioglu, M.J. Givens, G. Mylonakis, J.P. Stewart, Evaluation of soil-structure interaction effects from system identification of structures subject to forced vibration tests. *Soil Dynamics and Earthquake Engineering*, 116, 747-760, 2019.
[34] F. de Silva, C. Amendola, D. Pitilakis, F. Silvestri, Comparisons among different techniques to derive the swaying and rocking stiffness and damping from field tests on a surface footing. (Submitted to *Journal of Geotechnical and Geoenvironmental Engineering*), 2021.
[35] A. Vratsikidis, D. Pitilakis, Soil mass participation in soil-structure interaction by field experiments in EuroProteas. Silvestri F., Moraci N. (Eds.). *Earthquake Geotechnical Engineering for Protection and Development of Environment and Constructions. London*: CRC Press, 2019. https://doi.org/10.1201/9780429031274.

[36] Gazetas G. Analysis of machine foundation vibrations: state of the art. *Soil Dynamics and Earthquake Engineering*, 2(1), 2-42, 1983.